

# Three-layer Aurivillius phases containing magnetic transition metal cations: $\text{Bi}_{2-x}\text{Sr}_{2+x}(\text{Nb},\text{Ta})_{2+x}\text{M}_{1-x}\text{O}_{12}$ , $\text{M} = \text{Ru}^{4+}$ , $\text{Ir}^{4+}$ , $\text{Mn}^{4+}$ , $x \approx 0.5$

Neeraj Sharma<sup>a</sup>, Chris D. Ling<sup>a,b,\*</sup>, Grant E. Wrighter<sup>a</sup>, Parry Y. Chen<sup>a</sup>,  
 Brendan J. Kennedy<sup>a</sup>, Peter L. Lee<sup>c</sup>

<sup>a</sup>School of Chemistry, The University of Sydney, Sydney, NSW 2006, Australia

<sup>b</sup>Bragg Institute, ANSTO, PMB 1, Menai, NSW 2234, Australia

<sup>c</sup>X-ray Operations and Research Division, Advanced Photon Source, Argonne National Laboratory, Argonne, IL 60439, USA

Received 13 September 2006; received in revised form 25 October 2006; accepted 27 October 2006

Available online 10 November 2006

## Abstract

We report the synthesis of Aurivillius-type phases incorporating magnetic  $\text{M}^{4+}$  cations ( $\text{M} = \text{Mn}, \text{Ru}, \text{Ir}$ ), based on the substitution of  $\text{M}^{4+}$  for  $\text{Ti}^{4+}$  in  $\text{Bi}_2\text{Sr}_2(\text{Nb},\text{Ta})_2\text{TiO}_{12}$ . The key to incorporating these magnetic transition metal cations appears to be the partial substitution of  $\text{Sr}^{2+}$  for  $\text{Bi}^{3+}$  in the  $\alpha\text{-PbO}$ -type layer of the Aurivillius phase, leading to a concomitant decrease in the  $\text{M}^{4+}$  content; i.e., the composition of the prepared compounds was  $\text{Bi}_{2-x}\text{Sr}_{2+x}(\text{Nb},\text{Ta})_{2+x}\text{M}_{1-x}\text{O}_{12}$ ,  $x \approx 0.5$ . These compounds only exist over a narrow range of  $x$ , between an apparent minimum ( $x \approx 0.4$ )  $\text{Sr}^{2+}$  content in the  $\alpha\text{-PbO}$ -type  $[\text{Bi}_2\text{O}_2]$  layer required for Aurivillius phases to form with magnetic  $\text{M}^{4+}$  cations, and an apparent maximum ( $x \approx 0.6$ )  $\text{Sr}^{2+}$  substitution in this  $[\text{Bi}_2\text{O}_2]$  layer. Rietveld-refinement of synchrotron X-ray powder diffraction data making use of anomalous dispersion at the Nb and Ru  $K$  edges show that the overwhelming majority of the incorporated  $\text{M}$  cations occupy the central of the three  $\text{MO}_6$  octahedral layers in the perovskite-type block. Magnetic susceptibility measurements are presented and discussed in the context of the potential for multiferroic (magnetoelectric) properties in these materials.

© 2006 Elsevier Inc. All rights reserved.

**Keywords:** Aurivillius phase; Rietveld-refinement; Multiferroic; Anomalous dispersion

## 1. Introduction

Aurivillius phases  $[\text{Bi}_2\text{O}_2] \cdots [\text{A}_{n-1}\text{B}_n\text{O}_{3n+1}]$  are layered oxides composed of  $\alpha\text{-PbO}$ -type layers  $[\text{Bi}_2\text{O}_2]^{2+}$  alternating with  $n$  perovskite-type layers [1,2]. Interest in Aurivillius phases has focused on their catalytic properties and oxygen ion conductivity, as well as their strong ferroelectricity [3,4] which arises due to the rotation of  $\text{BO}_6$  octahedra, lowering the symmetry from tetragonal to orthorhombic or monoclinic, and allowing the perovskite  $A$ - and  $B$ -site cations to be displaced relative to the oxygen anion array.

\*Corresponding author. School of Chemistry, The University of Sydney, Sydney, NSW 2006, Australia. Fax: +61 2 9351 3329.

E-mail address: [c.ling@chem.usyd.edu.au](mailto:c.ling@chem.usyd.edu.au) (C.D. Ling).

Substituting magnetic transition metal cations into the central octahedral layer of the perovskite-type block, while maintaining ferroelectric displacements in the outer octahedral layers, presents a possible route to multiferroic (magnetoelectric) materials. The desired crystallographically ordered layering of magnetic and non-magnetic transition metal  $\text{MO}_6$  octahedra is certainly more likely to be achieved in a naturally layered perovskite such as this than in a conventional 3D perovskite, where such layering generally requires a lowering of symmetry. However, there have been few reports of Aurivillius phases that contain magnetic transition metal cations, which do not appear to form easily. Most of these concern high-order Aurivillius phases ( $n \geq 4$ ) such as  $\text{Bi}_5\text{Ti}_3\text{FeO}_{15}$ , which have a strong propensity for stacking faults [5] and  $B$ -site disorder [6,7], making long-range-ordered magnetism unlikely.

Three-layer ( $n = 3$ ) Aurivillius phases have the greatest contrast between the coordination environments of the *B*-site cations in the central and outer octahedral layers of the perovskite-type block, maximizing the potential for layered *B*-site ordering; although considerable *B*-site disorder is still observed, e.g., between Nb and Ti in  $\text{Bi}_2\text{Sr}_2\text{Nb}_2\text{TiO}_{12}$  [8]. Previous reports of magnetic  $n = 3$  Aurivillius phases are contradictory. Yu et al. [9] reported the synthesis of  $\text{Bi}_2\text{Sr}_2\text{Nb}_2\text{MnO}_{12}$ , i.e., the complete substitution of  $\text{Mn}^{4+}$  for  $\text{Ti}^{4+}$  in  $\text{Bi}_2\text{Sr}_2\text{Nb}_2\text{TiO}_{12}$ , presenting (but not refining) X-ray powder diffraction (XRD) data. McCabe and Greaves [10] could not reproduce this phase in the manner reported, observing an impurity phase in neutron powder diffraction (NPD) data, and proposing a single-phase sample of composition  $\text{Bi}_2\text{La}_{0.6}\text{Sr}_{1.4}\text{Nb}_2\text{MnO}_{12}$  (in which Mn has an average valence state of 3.4). Nevertheless, both groups of authors did present evidence for the preferential occupation of the central perovskite *B*-sites by Mn, and the outer *B*-sites by Nb.

Here we report the synthesis, structural and physical property characterization of a series of phases  $\text{Bi}_{2-x}\text{Sr}_{2+x}(\text{Nb},\text{Ta})_{2+x}(\text{Ru},\text{Ir},\text{Mn})_{1-x}\text{O}_{12}$  which offers an alternative model of  $\text{Mn}^{4+}$ -containing Aurivillius phases to those of both Yu et al. [9] and McCabe and Greaves [10], as well as representing the first incorporation of  $\text{Ru}^{4+}$  and  $\text{Ir}^{4+}$  into Aurivillius phases.

## 2. Experimental

Polycrystalline samples of  $\text{Bi}_{2-x}\text{Sr}_{2+x}B_{2+x}M_{1-x}\text{O}_{12}$ , where  $B = \text{Nb}, \text{Ta}$  and  $M = \text{Ru}, \text{Ir}, \text{Mn}$  were prepared over a range of  $x$  by conventional solid state synthesis using stoichiometric quantities of  $\text{Bi}_2\text{O}_3$  (Aithaca, 99.999%),  $\text{RuO}_2$  (Aithaca, 99.99%),  $\text{IrO}_2$  (Aithaca, 99.99%),  $\text{SrCO}_3$  (Aithaca, 99.995%),  $\text{Mn}_2\text{O}_3$  (Aldrich, 99.999%),  $\text{Nb}_2\text{O}_5$  (Aldrich, 99.99%), and  $\text{Ta}_2\text{O}_5$  (Aldrich, 99.99%). Reagents were mixed, ground and pre-heated for 1 h at 850 °C. For each composition, approximately half of the sample volume was then pressed into a pellet and heated in cycles of 950 °C for 100 h, 1000 °C for 50 h, and

1050 °C for 50 h, with intermediate regrinding, until a single phase was observed by XRD. The remaining half of the sample was used as a ‘sacrificial’ powder to bury the pellets, in order to minimize the loss of  $\text{Bi}_2\text{O}_3$  through volatilization.

Laboratory XRD data were collected on a Shimadzu XRD-6000 using  $\text{Cu K}\alpha$  radiation. A Philips XL30 scanning electron microscope (SEM) was used to carry out energy dispersive X-ray spectroscopy (EDS).

Synchrotron XRD data were collected on the X-ray Operations and Research (XOR) beamline 1-BM-C at the Advanced Photon Source (APS), Argonne National Laboratory, using flat plate geometry at wavelengths of 0.6584, 0.5586, and 0.5920 Å. NPD data were collected on the High Resolution Powder Diffractometer (HRPD) at the High-Flux Australian Reactor (HIFAR) facility, Australian Nuclear Science and Technology Organisation (ANSTO), Lucas Heights Science and Technology Centre, Australia. Rietveld-refinements were carried out using the GSAS [11] suite of programs with the EXPGUI [12] frontend.

Magnetic property measurements were carried out on a Physical Properties Measurement System (PPMS) (Quantum Design) using the DC extraction method in an applied magnetic field of 10,000 Oe. In order to avoid the preferential alignment of these strongly anisotropic layered phases in the applied magnetic field, the samples were mixed with a small quantity of Vaseline<sup>TM</sup>.

## 3. Results

Initial attempts to synthesize stoichiometric samples of  $\text{Bi}_2\text{Sr}_2\text{Nb}_2\text{RuO}_{12}$  and  $\text{Bi}_2\text{Sr}_2\text{Nb}_2\text{MnO}_{12}$  following the synthetic strategy of Yu et al. [9] resulted in multi-phase products. For  $\text{Bi}_2\text{Sr}_2\text{Nb}_2\text{RuO}_{12}$ , we observed that lattice parameters of the dominant phase, as determined by XRD, were very close to those of the strontium-excess  $n = 3$  Aurivillius phase [8]  $\text{Bi}_{2-x}\text{Sr}_{2+x}\text{Nb}_{2+x}\text{Ti}_{1-x}\text{O}_{12}$  ( $0 < x < 0.8$ ) at  $x \approx 0.5$ . Repeating the synthesis at a nominal composition  $\text{Bi}_{2-x}\text{Sr}_{2+x}\text{Nb}_{2+x}\text{Ru}_{1-x}\text{O}_{12}$ ,  $x = 0.5$ , led to a single-phase sample by XRD. The synthesis was then repeated at a range

Table 1

Summary of key data for  $\text{Bi}_{2-x}\text{Sr}_{2+x}B_{2+x}M_{1-x}\text{O}_{12}$  obtained by Rietveld-refinement of synchrotron XRD data, including: empirical bond valence sums on the mixed *B/M*(2) site at (0.5, 0.5, 0.5); the nominal fraction ( $x$ ) of *B* on this mixed site, compared to  $x$  as determined by Rietveld-refinement of synchrotron XRD data and by EDS (based on both the Bi:Sr and *B:M* ratios); and the unit cell parameters

<i>B</i>	Nb	Ta	Nb	Ta	Nb	Ta
BVS <i>B</i> (2)	5.14	5.32	5.20	—	4.86	—
<i>M</i>	Ru	Ru	Mn	Mn	Ir	Ir
BVS <i>M</i> (2)	4.17	4.21	3.39	—	4.92	—
$x$ (nominal)	0.5	0.4	0.4	0.5	0.5	0.5
$x$ (XRD) Bi:Sr	0.654(4)	0.652(4)	0.544(3)	—	0.570(4)	—
$x$ (XRD) <i>B:M</i>	0.601(18)	0.641(6)	0.665(8)	—	0.767(3)	—
$x$ (EDS) Bi:Sr	0.6(1)	—	0.5(1)	—	0.5(2)	—
$x$ (EDS) <i>B:M</i>	0.4(1)	—	0.4(2)	—	0.7(2)	—
$a$ (Å)	3.921698(12)	3.918098(13)	3.926331(18)	3.92442(4)	3.921685(13)	3.917858(19)
$c$ (Å)	33.6415(2)	33.5555(2)	33.4103(3)	33.6990(9)	33.7618(2)	33.8358(5)
$V$ (Å <sup>3</sup> )	517.394(4)	515.127(6)	515.056(8)	519.00(2)	519.244(6)	519.366(10)

of  $x$ , however, the range over which single-phase samples could be produced proved to be extremely narrow,  $0.45 < x < 0.6$ . Samples of the Ta (for Nb) analogue  $\text{Bi}_{2-x}\text{Sr}_{2+x}\text{Ta}_{2+x}\text{Ru}_{1-x}\text{O}_{12}$ ,  $0.3 < x < 0.5$ , were subsequently prepared in the same manner. The same approach was used to synthesize samples of  $\text{Bi}_{2-x}\text{Sr}_{2+x}\text{Nb}_{2+x}\text{Mn}_{1-x}\text{O}_{12}$ ,  $0.3 < x < 0.5$ ,  $\text{Bi}_{2-x}\text{Sr}_{2+x}\text{Ta}_{2+x}\text{Mn}_{1-x}\text{O}_{12}$ ,  $0.4 < x < 0.6$ ,  $\text{Bi}_{2-x}\text{Sr}_{2+x}\text{Nb}_{2+x}\text{Ir}_{1-x}\text{O}_{12}$ ,  $0.45 \leq x \leq 0.6$ , and  $\text{Bi}_{2-x}\text{Sr}_{2+x}\text{Ta}_{2+x}\text{Ir}_{1-x}\text{O}_{12}$ ,  $0.45 \leq x \leq 0.55$ .

Samples were analyzed by EDS to confirm their compositions. For a representative sample of  $\text{Bi}_{2-x}\text{Sr}_{2+x}\text{B}_{2+x}\text{M}_{1-x}\text{O}_{12}$

where  $B = \text{Nb}$ ,  $\text{Ta}$  and  $M = \text{Ru}$ ,  $\text{Mn}$ , and  $\text{Ir}$ , 10 or more crystallites were examined and  $x$  was determined independently based on the ratio of Bi:Sr and on the ratio of  $B:M$ . Where  $B = \text{Nb}$ , both these ratios indicated  $x$  values within error of the nominal value from synthesis. Results are summarized in Table 1, and will be discussed further in the context of the other data in Table 1 in Section 4 (Discussion) below. Where  $B = \text{Ta}$ , the close overlap of Ta and Sr  $M$  emission lines unfortunately rendered both ratios extremely unreliable, and these results are not reported.

Synchrotron XRD data were collected in order to unambiguously determine the  $B$ -site ordering in the perovskite block. The most thoroughly characterized sample was  $\text{Bi}_{2-x}\text{Sr}_{2+x}\text{Nb}_{2+x}\text{Ru}_{1-x}\text{O}_{12}$ ,  $x = 0.5$ , for which data were collected at wavelengths below the Nb  $K$  edge (0.6584 Å), above the Ru  $K$  edge (0.5586 Å), and in between (0.5920 Å). All three patterns were Rietveld-refined simultaneously, after being truncated at different angles in order to obtain the same maximum  $\sin \theta/\lambda$ . Anisotropic strain and preferred orientation (March-Dollase [13,14], with the (001) plane perpendicular to the layer-stacking axis  $c$  refining to  $\sim 85\%$  intensity) were included in the refinement. Because there are four crystallographically distinct cation sites with (potentially) mixed occupancies involving cations of different charge, it was not possible to refine all these occupancies simultaneously while constraining the overall composition to be chemically reasonable. Initial refinements used no constraints between sites, and indicated that the overall composition was indeed very close to that expected on the basis of synthesis and supported by EDS (Table 1). The overall composition was subsequently constrained to  $\text{Bi}_{1.5}\text{Sr}_{2.5}\text{Nb}_{2.5}\text{Ru}_{0.5}\text{O}_{12}$ , while allowing the compositions of individual sites to vary, in the

Table 2  
Final parameters for  $\text{Bi}_{2-x}\text{Sr}_{2+x}\text{Nb}_{2+x}\text{Ru}_{1-x}\text{O}_{12}$ ,  $x = 0.5$ , from simultaneous Rietveld-refinement of synchrotron XRD data collected at 0.6584, 0.5920, and 0.5586 Å

Site	$x$	$y$	$z$	Occupancy	$100U_{\text{iso}}$
Bi(1)	0.5	0.5	0.06236(2) <sup>1</sup>	0.039(1) <sup>2</sup>	1.14(3) <sup>3</sup>
Sr(1)	0.5	0.5	0.06236(2) <sup>1</sup>	0.961(1) <sup>−2</sup>	1.14(3) <sup>3</sup>
Bi(2)	0.5	0.5	0.21624(2)	0.711(1) <sup>−2</sup>	0.49(2) <sup>4</sup>
Sr(2)	0.5	0.5	0.20341(11)	0.289(1) <sup>2</sup>	0.49(2) <sup>4</sup>
Ru(1)	0.5	0.5	0.5	0.492(12) <sup>5</sup>	1.08(4) <sup>6</sup>
Nb(1)	0.5	0.5	0.5	0.508(12) <sup>−5</sup>	1.08(4) <sup>6</sup>
Ru(2)	0.5	0.5	0.37367(2) <sup>7</sup>	0.004(6) <sup>−5</sup>	1.24(5) <sup>8</sup>
Nb(2)	0.5	0.5	0.37367(2) <sup>7</sup>	0.996(6) <sup>5</sup>	1.24(5) <sup>8</sup>
O(1)	0.5	0	0.5	1	4.5(2)
O(2)	0.5	0	0.25	1	4.1(2)
O(3)	0.5	0.5	0.44105(11)	1	1.46(14)
O(4)	0.5	0.5	0.31726(16)	1	6.0(2)
O(5)	0.5	0	0.11591(8)	1	0.72(8)

Space group  $I4/mmm$  (#139),  $a = 3.921698(12)$  Å,  $c = 33.6415(2)$  Å. Goodness-of-fit = 1.33 for 94 refined parameters. Overall powder  $R$ -factors:  $R_p = 0.0910$ ,  $wR_p = 0.1200$ . Italicized superscript numbers indicate constraints.

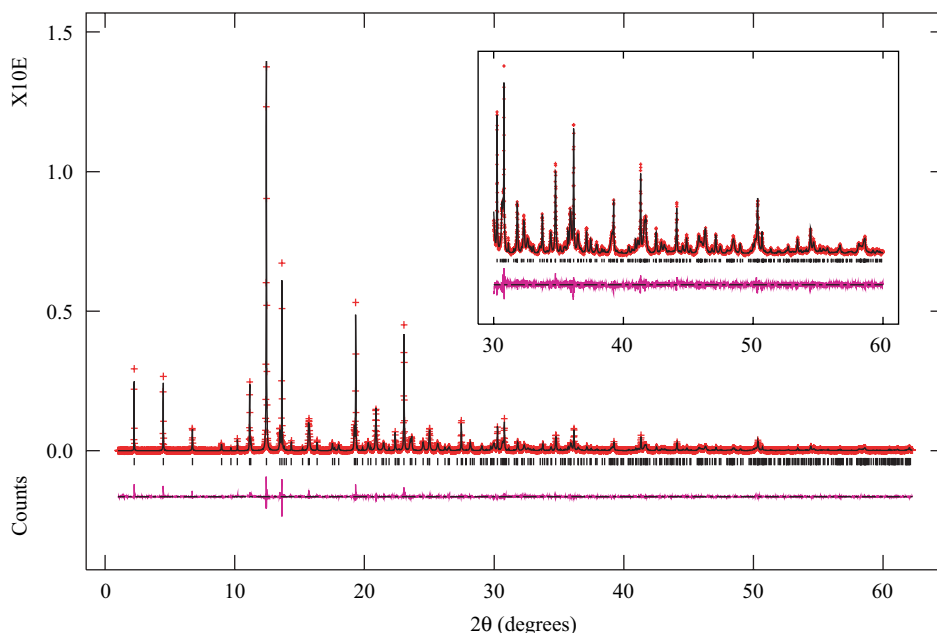


Fig. 1. Final fit to Rietveld-refined  $\lambda = 6584$  Å synchrotron XRD data for  $\text{Bi}_{2-x}\text{Sr}_{2+x}\text{Nb}_{2+x}\text{Ru}_{1-x}\text{O}_{12}$ ,  $x = 0.5$ . Observed data are shown at crosses (+), calculated data as a solid line, and the difference as a solid line below. Data in the range  $30 \leq 2\theta \leq 60$ ° are shown rescaled above in order to emphasize the amount of information contained in this data. Goodness of fit = 1.33 for 94 refined parameters. Overall powder  $R$ -factors:  $R_p = 0.0910$ ,  $wR_p = 0.1200$ .

manner indicated by the italicized superscript symbols in Table 2. Mixed sites were constrained to the same positions, with the exception of Bi(2)/Sr(2), where Sr<sup>2+</sup> cations doped into the Bi<sub>2</sub>O<sub>2</sub> layer were allowed to move closer to the perovskite-type block because they lack the stereochemically-active 6s<sup>2</sup> lone-pair of Bi<sup>3+</sup>. (This effect was also observed by Hervoches and Lightfoot for Bi<sub>2-x</sub>Sr<sub>2+x</sub>Nb<sub>2+x</sub>Ti<sub>1-x</sub>O<sub>12</sub> [8]). The final fit to observed data for  $\lambda = 0.6584 \text{ \AA}$  is shown in Fig. 1, final Rietveld-refined parameters are presented in Table 2, and the structure is shown in Fig. 2. Note that the overwhelming majority of the additional Sr<sup>2+</sup> due to  $x$  is located on the

Bi/Sr(2) site (in the  $\alpha$ -PbO-type layer) while the Bi/Sr(1) site (the *A*-site in the perovskite-type block) remains almost exclusively occupied by Sr<sup>2+</sup>; and that the overwhelming majority of the additional Nb<sup>5+</sup> due to  $x$  was located on the Nb/Ru(1) site (the *B*-site of the central octahedral layer of the perovskite-type block) while the Nb/Ru(2) site (the *B*-site of outer octahedral layer) remained almost exclusively occupied by Nb<sup>5+</sup> (see Fig. 2).

Synchrotron XRD data were collected for Bi<sub>2-x</sub>Sr<sub>2+x</sub>Ta<sub>2+x</sub>Ru<sub>1-x</sub>O<sub>12</sub>,  $x = 0.4$ , below (0.5920  $\text{\AA}$ ) and above (0.5586  $\text{\AA}$ ) the Ru *K* edge; and for the remaining niobium-containing samples (Bi<sub>2-x</sub>Sr<sub>2+x</sub>Nb<sub>2+x</sub>Mn<sub>1-x</sub>O<sub>12</sub>,  $x = 0.4$ , and Bi<sub>2-x</sub>Sr<sub>2+x</sub>Nb<sub>2+x</sub>Ir<sub>1-x</sub>O<sub>12</sub>,  $x = 0.5$ ) below (0.6584  $\text{\AA}$ ) and above (0.5920  $\text{\AA}$ ) the Nb *K* edge. For all of these samples, data collected at different wavelengths were Rietveld-refined simultaneously in the manner described above for Bi<sub>2-x</sub>Sr<sub>2+x</sub>Nb<sub>2+x</sub>Ru<sub>1-x</sub>O<sub>12</sub>,  $x = 0.5$ . Synchrotron XRD data for the remaining two samples (Bi<sub>2-x</sub>Sr<sub>2+x</sub>Ta<sub>2+x</sub>Mn<sub>1-x</sub>O<sub>12</sub>,  $x = 0.5$ , and Bi<sub>2-x</sub>Sr<sub>2+x</sub>Ta<sub>2+x</sub>Ir<sub>1-x</sub>O<sub>12</sub>,  $x = 0.5$ ) were collected at 0.6584  $\text{\AA}$  only and Rietveld-refined in the manner described above for Bi<sub>2-x</sub>Sr<sub>2+x</sub>Nb<sub>2+x</sub>Ru<sub>1-x</sub>O<sub>12</sub>,  $x = 0.5$ . For the *B* = Ta, *M* = Mn sample, a small impurity revealed by synchrotron XRD data could not be identified. For the *B* = Ta, *M* = Ir sample, synchrotron XRD data revealed that the reaction was not 100% complete; impurities were identified as 15 wt% Sr<sub>5</sub>Ta<sub>4</sub>O<sub>15</sub> (isostructural with Sr<sub>5</sub>Nb<sub>4</sub>O<sub>15</sub> [15]) and 5 wt% Bi<sub>2</sub>Ir<sub>2</sub>O<sub>7</sub> [16], and included in the refinement. In all cases, the refinement of cation occupancies indicated that the overwhelming majority of the additional Sr<sup>2+</sup> due to  $x$  was located on the Bi/Sr(2) site while the Bi/Sr(1) site remained almost exclusively occupied by Sr<sup>2+</sup>, and the overwhelming majority of the additional B<sup>5+</sup> due to  $x$  was located on the *B/M*(1) site while the *B/M*(2) site remained almost exclusively occupied by B<sup>5+</sup>.

Based on the above evidence that the cation doping concerns almost exclusively the Bi/Sr(2) and *B/M*(1) sites, the synchrotron XRD data were re-refined allowing the compositions of those two sites to vary independently of one another. This provided two independent values for  $x$ ; one based on the Bi:Sr ratio (i.e. Bi<sub>2-x</sub>Sr<sub>2+x</sub>) and one based on the *B*:*M* ratio (i.e. B<sub>2+x</sub>M<sub>1-x</sub>). These results are presented in Table 1, along with the refined lattice parameters. Note that for the two samples that contained impurities (*B* = Ta, *M* = Ir and *B* = Ta, *M* = Mn), the refinement of compositions in this manner was found to be unstable and the results are not reported.

Room-temperature NPD data were collected for the Bi<sub>2-x</sub>Sr<sub>2+x</sub>(Nb/Ta)<sub>2+x</sub>(Ru/Mn)<sub>1-x</sub>O<sub>12</sub> samples and Rietveld-refined in I4/mmm. No evidence was seen for symmetry lowering, even though careful attention was paid to the low-angle peaks for evidence of splitting as recently observed by Zhou et al. [17]. Refinement of oxygen atom occupancies found no statistically significant evidence for vacancies, as expected for Aurivillius phases with  $n > 1$  [7]. Final Rietveld-refined parameters are not presented but were generally within error of those obtained using

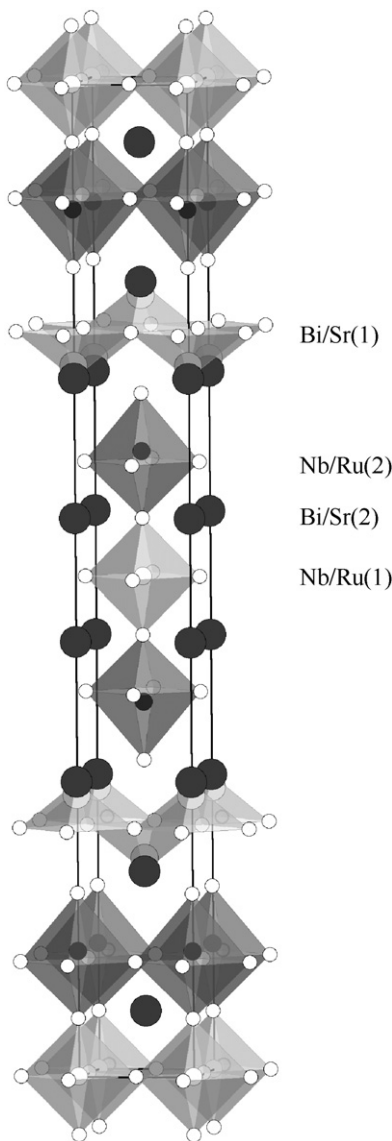


Fig. 2. Polyhedral representation of the final Rietveld-refined structure from synchrotron XRD data at 300 K of Bi<sub>2-x</sub>Sr<sub>2+x</sub>Nb<sub>2+x</sub>Ru<sub>1-x</sub>O<sub>12</sub>,  $x = 0.5$ . BiO<sub>4</sub> square pyramids are drawn in light gray, NbO<sub>6</sub> octahedra in dark gray, and mixed (Nb,Ru)O<sub>6</sub> octahedra in light gray. Sr cations are drawn as dark gray spheres. O anions are drawn as white spheres. Note that slightly offset Bi and Sr positions on the split Bi/Sr(1) site, vs. the perfectly overlapped Bi and Sr positions on the Bi/Sr(2) site (drawn as dark gray spheres).

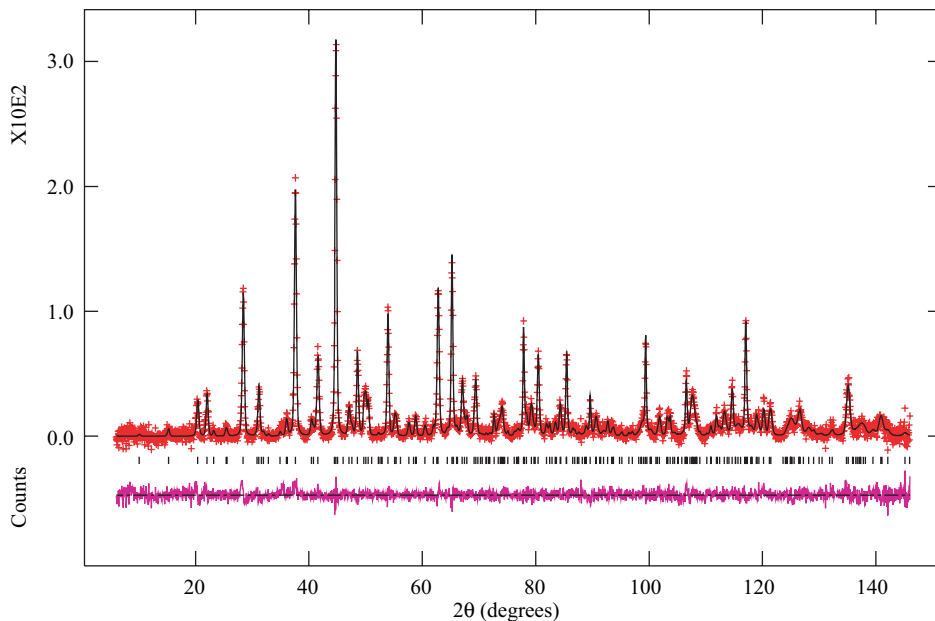


Fig. 3. Final fit to Rietveld-refined  $\lambda = 1.49 \text{ \AA}$  NPD data for  $\text{Bi}_{2-x}\text{Sr}_{2+x}\text{Nb}_{2+x}\text{Ru}_{1-x}\text{O}_{12}$ ,  $x = 0.5$ . Observed data are shown at crosses (+), calculated data as a solid line, and the difference as a solid line below. Goodness-of-fit = 4.301 for 54 refined parameters. Overall powder  $R$ -factors:  $R_p = 0.0850$   $wR_p = 0.0574$ .

synchrotron XRD, the results of which were found to be more precise in this case. The final fit to observed data for  $\text{Bi}_{2-x}\text{Sr}_{2+x}\text{Nb}_{2+x}\text{Ru}_{1-x}\text{O}_{12}$ ,  $x = 0.5$ , is shown in Fig. 3. Low-temperature NPD data ( $T = 6 \text{ K}$ ) were also collected and Rietveld-refined, but no evidence was found for either symmetry-lowering or long-range magnetic ordering.

Magnetic susceptibility data were collected for all samples. Plots of inverse susceptibility *vs.* temperature are shown in Fig. 4.

#### 4. Discussion

The incorporation of magnetic transition metals into the  $n = 3$  Aurivillius phase  $\text{Bi}_2\text{Sr}_2\text{Nb}_2\text{TiO}_{12}$  was first reported by Yu et al. [9], based on the complete substitution of  $\text{Mn}^{4+}$  for  $\text{Ti}^{4+}$ , i.e.,  $\text{Bi}_2\text{Sr}_2\text{Nb}_2\text{MnO}_{12}$ . McCabe and Greaves [10] could not reproduce this phase at the reported stoichiometry without significant  $\text{Sr}(\text{Nb}, \text{Mn})\text{O}_3$  and  $\text{Bi}_2\text{O}_3$  impurities, and suggested on the basis of Rietveld-refinement against NPD data that the true stoichiometry was  $\text{Bi}_{2.8}\text{Sr}_{1.2}\text{Nb}_{2.34}\text{Mn}_{0.66}\text{O}_{12}$  (implying an average oxidation state for Mn of 2.27). Our results for the incorporation of  $\text{Ru}^{4+}$ , the oxidation state of which is quite certain, and our subsequent preparation of analogous  $\text{Mn}^{4+}$  and  $\text{Ir}^{4+}$  phases, suggest a third possibility for the Mn-doped phase, namely  $\text{Bi}_{2-x}\text{Sr}_{2+x}\text{Nb}_{2+x}\text{Mn}_{1-x}\text{O}_{12}$ ,  $x \approx 0.5$ . Our formulation gives an Nb:Mn ratio close to that refined against NPD data by McCabe and Greaves, but quite a different Bi:Sr ratio; this discrepancy should be considered in light of the much stronger contrast between neutron scattering cross-sections of Nb (6.25) and Mn (2.15), compared to the contrast between Bi (9.16) and Sr (6.25).

Our formulation of the phases synthesized in this study as  $\text{Bi}_{2-x}\text{Sr}_{2+x}\text{B}_{2+x}\text{M}_{1-x}\text{O}_{12}$  ( $\text{B} = \text{Nb}, \text{Ta}; \text{M} = \text{Ru}, \text{Mn}, \text{Ir}$ ) is consistent with the data presented by Hervoches and Lightfoot [8] for  $\text{Bi}_{2-x}\text{Sr}_{2+x}\text{Nb}_{2+x}\text{Ti}_{1-x}\text{O}_{12}$ , in which the additional  $\text{Sr}^{2+}$  is substituted for  $\text{Bi}^{3+}$  in the  $\alpha$ -PbO-type  $\text{Bi}_2\text{O}_2$  layer, requiring a concomitant substitution of additional  $\text{Nb}^{5+}$  for  $\text{Ti}^{4+}$  in the perovskite-type layer for charge balance (note that  $n > 1$  Aurivillius phases cannot tolerate oxygen vacancies [18].) This interpretation is supported in four different ways, summarized in Table 1: firstly, single-phase samples (except for  $\text{B} = \text{Ta}$  and  $\text{M} = \text{Mn}, \text{Ir}$ ) could be obtained at those stoichiometries; secondly, the lattice parameters are all expanded relative to those of the parent ( $x = 0$ ) phases  $\text{Bi}_2\text{Sr}_2\text{B}_2\text{TiO}_{12}$ , and suggest  $x \approx 0.5$  (see [8], Fig. 5); thirdly, Rietveld-refined values of  $x$  based on both Bi:Sr and  $\text{B}:M$  ratios, using synchrotron XRD data at multiple wavelengths around the Nb and Ru  $K$  edges; and fourthly, values of  $x$  obtained by EDS based on both Bi:Sr and  $\text{B}:M$  ratios. While there is some small variation in  $x$  as determined by these different methods, Table 1 nevertheless presents compelling evidence for the existence of Aurivillius phases of general composition  $\text{Bi}_{2-x}\text{Sr}_{2+x}\text{B}_{2+x}\text{M}_{1-x}\text{O}_{12}$  ( $\text{B} = \text{Nb}, \text{Ta}; \text{M} = \text{Ru}, \text{Mn}, \text{Ir}; x \approx 0.5$ ).

In the case of the  $\text{M} = \text{Mn}$  phases, these results are notable as they clearly support the presence of  $\text{Mn}^{4+}$  within the perovskite-type layer of Aurivillius phases. Furthermore, Rietveld-refinements against synchrotron XRD data (using anomalous dispersion to maximize the contrast between metal atoms species) very strongly suggest that all this  $\text{Mn}^{4+}$  is located in the central octahedral layer of the perovskite-type block, which is therefore  $\sim 50\%$   $\text{Mn}^{4+}$  and  $\sim 50\%$   $\text{B}^{5+}$ . Previous

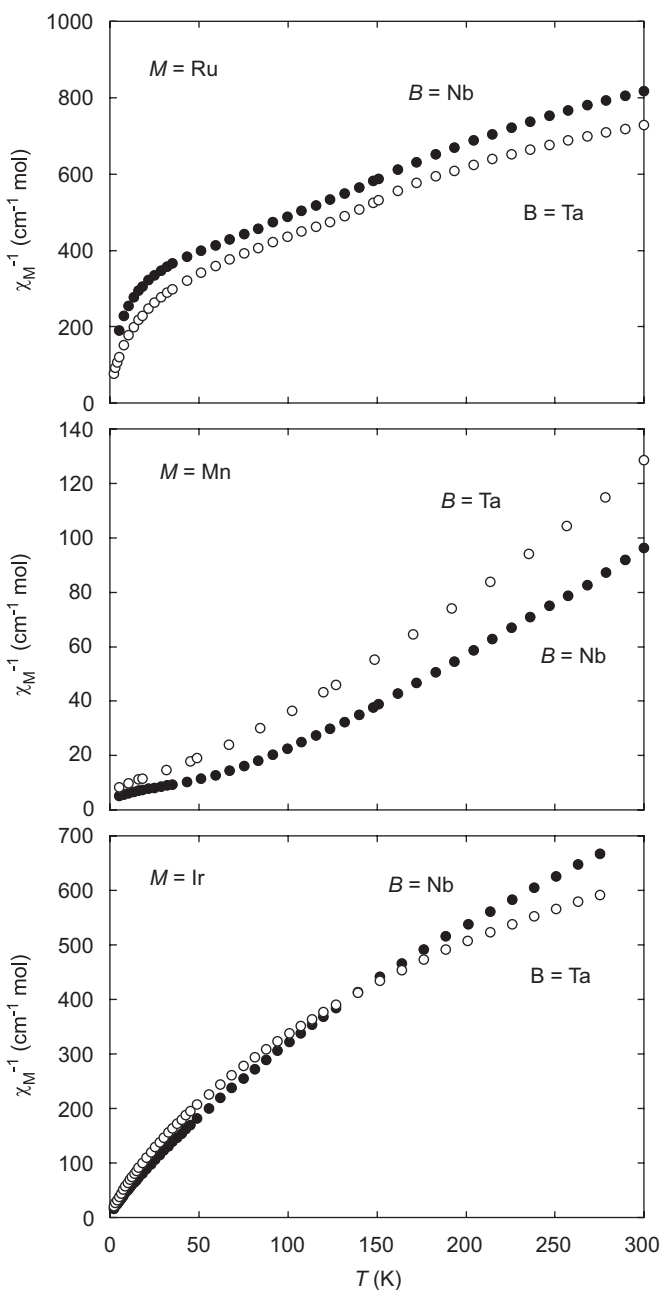


Fig. 4. Plots of inverse magnetic susceptibility vs. temperature for Aurivillius phases containing Ru(IV) (top), Mn(IV) (middle), and Ir(IV) (bottom).  $B = \text{Nb}$  data are plotted as solid circles, and  $B = \text{Ta}$  data are plotted as open circles.

considerations of the perovskite-type block in Aurivillius phases by Armstrong and Newnham [19] concluded that the  $B$ -site could only accommodate transition metals with effective ionic radii ( $IR$ ) [20] in the range  $0.58 \leq IR \leq 0.65 \text{ \AA}$ .  $\text{Mn}^{4+}$  ( $IR = 0.53 \text{ \AA}$ ) falls outside of this range, whereas  $\text{Ru}^{4+}$  ( $IR = 0.62 \text{ \AA}$ ) and  $\text{Ir}^{4+}$  ( $IR = 0.625 \text{ \AA}$ ) fall inside it, as do  $\text{Ti}^{4+}$  ( $IR = 0.60 \text{ \AA}$ ) and  $\text{Nb}^{5+}$  ( $IR = 0.64 \text{ \AA}$ ). Empirical bond valence sums [21] presented in Table 1 for  $B$  and  $M$  cations on the mixed  $B/M(2)$  site are within the normally encountered range for  $\text{Nb}^{5+}$ ,  $\text{Ta}^{5+}$ , and  $\text{Ru}^{4+}$ , although they indicate that  $\text{Mn}^{4+}$  is

somewhat underbonded while  $\text{Ir}^{4+}$  is somewhat overbonded. (Note that for the  $\text{Ta}/\text{Mn}$  and  $\text{Ta}/\text{Ir}$  samples, the presence of impurities made the position of  $\text{O}(3)$  insufficiently well determined by Rietveld-refinement for reliable bond valence sums to be obtained.)

The archetype  $B = \text{Nb}$ ,  $M = \text{Ti}$  phase  $\text{Bi}_{2-x}\text{Sr}_{2+x}\text{Nb}_{2+x}\text{Ti}_{1-x}\text{O}_{12}$  [8] was reported to be stable in the range  $0 \leq x \leq 0.6$ , with a second phase  $\text{Bi}_5\text{Nb}_3\text{O}_{15}$  appearing at higher  $x$ . In the present study, where  $M = \text{Ru}$ ,  $\text{Mn}$ , and  $\text{Ir}$ , the stable ranges are all approximately  $0.4 \leq x \leq 0.6$ . The upper limit, which implies the maximum amount of  $\text{Sr}^{2+}$  that can be doped into the  $\text{Bi}_2\text{O}_2$  layer, remains the same; and the lower limit implies the minimum amount of  $\text{Sr}^{2+}$  doping required before these particular  $M$  cations can be incorporated into the Aurivillius structure. The exact mechanism by which  $\text{Sr}^{2+}$  doping in the  $\text{Bi}_2\text{O}_2$  layer permits the incorporation of these  $M$  cations is unclear, but presumably related to the increased unit cell volume that it elicits. We are presently investigating means by which to reduce this lower limit. Given the results from Rietveld-refinement against synchrotron XRD data show that the overwhelming majority of  $M$  cations are located on the central octahedral layer of the perovskite-type block, reducing  $x$  to 0 should produce a complete layer of magnetically active transition metal cations, presenting the possibility of long-range magnetic order.<sup>1</sup>

Although no evidence was seen for long-range magnetic order in the low-temperature NPD data, the magnetic susceptibility data presented in Fig. 4 indicate that the presence of  $\sim 50\%$  magnetic cations in this central layer does lead to some short-range magnetic interactions. For the larger  $M = \text{Ru}$  and  $\text{Ir}$ , spin-orbit coupling dominates, but for  $M = \text{Ru}$  there is nevertheless an indication of antiferromagnetic exchange interactions at low temperature; and for  $M = \text{Mn}$ , these data provide evidence for ferromagnetic exchange with quite low Curie temperatures  $T_C \approx 50 \text{ K}$  ( $B = \text{Nb}$ ) and  $T_C \approx 25 \text{ K}$  ( $B = \text{Ta}$ ).

Given that this investigation was driven by the search for multiferroic (ferroelectromagnetic) Aurivillius phases, the observation that these oxides are tetragonal  $I4/mmm$  rather than orthorhombic  $B2ab$  [16] is worthy of discussion. Ferroelectricity in Aurivillius phases arises due to a polar displacement of cations that is often accompanied by a rotation of  $\text{BO}_6$  octahedra in the perovskite-type block. This rotation is due to a size mismatch between the perovskite-type  $A$ - and  $B$ -site cations, where the  $B$ -site cation is larger than optimal. Comparing the orthorhombic parent compound  $\text{Bi}_2\text{Sr}_2\text{Nb}_2\text{TiO}_{12}$  to the tetragonal

<sup>1</sup>While the present work was in review, a report appeared [22] of the synthesis of the  $x = 0$  member of this series, i.e.,  $\text{Bi}_2\text{Sr}_2\text{Nb}_2\text{RuO}_{12}$ , under effectively identical synthetic conditions to those utilized in the present study. However, the report is based on laboratory XRD data alone, and no Rietveld refinements were performed. This would have made it difficult to identify the low- $x$  impurities  $\text{Sr}(\text{Nb},\text{Mn})\text{O}_3$  and  $\text{Bi}_2\text{O}_3$ , which have closely related structures, similar unit cell dimensions, and hence significant XRD peak overlap with the Aurivillius-type phase under consideration.

$\text{Bi}_{1.5}\text{Sr}_{2.5}\text{Nb}_{2.5}\text{Ru}_{0.5}\text{O}_{12}$ ,  $\text{Ti}^{4+}$  ( $IR = 0.605 \text{ \AA}$ ) on the central perovskite-type  $B$ -site is replaced by 50 %  $\text{Ru}^{4+}$  ( $IR = 0.62$ ) and 50 %  $\text{Nb}^{5+}$  ( $IR = 0.68$ ), with an average size  $IR = 0.65 \text{ \AA}$ .<sup>2</sup> This substitution should therefore increase the magnitude of the octahedral rotation, however, the (121) NPD peak that characterizes orthorhombic symmetry-lowering in  $\text{Bi}_2\text{Sr}_2\text{Nb}_2\text{TiO}_{12}$  [16] was not observed for  $\text{Bi}_{1.5}\text{Sr}_{2.5}\text{Nb}_{2.5}\text{Ru}_{0.5}\text{O}_{12}$ . In the case of  $\text{Bi}_{1.5}\text{Sr}_{2.5}\text{Nb}_{2.5}\text{Mn}_{0.5}\text{O}_{12}$  the average size of the perovskite-type  $B$ -site cation is  $(0.68 + 0.53)/2 = 0.605 \text{ \AA}$  which is identical to that of  $\text{Ti}^{4+}$ , but again, the (121) NPD peak was not observed. The absence of orthorhombic symmetry-lowering, and hence ferroelectricity, in these new oxides is therefore due to factors other than ionic radii. It may in fact be due to the presence of unpaired  $d$ -electrons on the perovskite-type  $B$ -site cations, a possibility that is discouraging in the context of the search for multiferroic Aurivillius phases.

## 5. Conclusions

We have presented evidence for the incorporation of  $\text{Ru}^{4+}$ ,  $\text{Ir}^{4+}$ , and  $\text{Mn}^{4+}$  into an  $n = 3$  Aurivillius phases of general composition  $\text{Bi}_{2-x}\text{Sr}_{2+x}(\text{Nb},\text{Ta})_{2+x}\text{M}_{1-x}\text{O}_{12}$ ,  $x \approx 0.5$ . The key feature of these phases is the partial substitution of  $\text{Sr}^{2+}$  for  $\text{Bi}^{3+}$  in the  $\alpha\text{-PbO}$ -type  $[\text{Bi}_2\text{O}_2]$  layer, which appears to be necessary for the incorporation of these magnetic transition metal cations in the perovskite-type layer. Rietveld-refinement of synchrotron XRD data using anomalous dispersion at the Nb and Ru  $K$  edges provides strong evidence that all these magnetic transition metal cations are located in the central octahedral layer of the perovskite-type block. Magnetic susceptibility measurements suggest short-range antiferromagnetic exchange interactions for  $M = \text{Ru}$  and ferromagnetic exchange interactions for  $M = \text{Mn}$ .

## Acknowledgments

The neutron powder diffraction work was supported by Australian Institute of Nuclear Science and Engineering

(AINSE) under AINGRA06246. The Advanced Photon Source (APS) is supported by the US Department of Energy, Office of Science, Basic Energy Sciences, under Contract No. W-31-109-Eng-38; and access to the APS for this project was supported by the Australian Synchrotron Research Program (ASRP) under 06/07-SRI-147. We wish to thank Drs. M.M. Elcombe and M. Avdeev of the Australian Nuclear Science and Technology Organisation (ANSTO) for collecting NPD data, and Dr. B. Moubarak of Monash University for collecting magnetic susceptibility data.

## References

- [1] B. Aurivillius, Ark. Kemi. 1 (1949) 463.
- [2] B. Aurivillius, Ark. Kemi. 2 (1950) 519.
- [3] E.C. Subbarao, J. Phys. Chem. Solids. 23 (1962) 665.
- [4] G.A. Smolenski, V.A. Isupov, A.I. Agranovskaya, Sov. Phys. Solid State (Engl. Transl.). 3 (1953) 651.
- [5] I.G. Ismailzade, V.I. Nesteren, F.A. Mirishli, P.G. Rustamov, Sov. Phys. Crystallogr. 12 (1967) 400.
- [6] C.H. Hervoches, A. Snedden, R. Riggs, S.H. Kilcoyne, P. Manuel, P. Lightfoot, J. Solid State Chem. 164 (2002) 280.
- [7] A. Snedden, C.H. Hervoches, P. Lightfoot, Phys. Rev. B. 67 (2003) 92102.
- [8] C.H. Hervoches, P. Lightfoot, J. Solid State Chem. 153 (2000) 66.
- [9] W.J. Yu, Y.I. Kim, D.H. Ha, J.H. Lee, Y.K. Park, S. Seong, N.H. Hur, Solid State Comm 111 (1999) 705.
- [10] E.E. McCabe, C. Greaves, J. Mater. Chem. 15 (2005) 177.
- [11] A.C. Larson, R.B. Von Dreele, Los Alamos National Laboratory Report LAUR 86-748, 1994.
- [12] B.H. Toby, J. Appl. Crystallogr. 34 (2001) 210.
- [13] A. March, Z. Kristallogr. 81 (1932) 285.
- [14] W.A. Dollase, J. Appl. Crystallogr. 19 (1986) 267.
- [15] N. Teneze, D. Mercurio, G. Trolliard, J.C. Champarnaud-Mesjard, Z. Kristallogr.-New Crystal Struct 215 (2000) 11.
- [16] B.J. Kennedy, J. Solid State Chem. 123 (1996) 14.
- [17] Q. Zhou, B. J. Kennedy, M. M. Elcombe, J. Solid State Chem. 2006, in press.
- [18] A. Snedden, S.M. Blake, P. Lightfoot, Solid State Ionics 156 (2003) 439.
- [19] R.A. Armstrong, R.E. Newnham, Mater. Res. Bull. 7 (1972) 1025.
- [20] R.D. Shannon, Acta Crystallogr. A 32 (1976) 751.
- [21] N.E. Brese, M. O'Keeffe, Acta Crystallogr. B 47 (1991) 192.
- [22] M. Tripathy, R. Mani, and J. Gopalakrishnan, Mater. Res. Bull. in press, doi:10.1016/j.materresbull.2006.08.009 (2006).

<sup>2</sup>Note that there is a competing, but much smaller, effect whereby increasing  $x$  leads to an increase in the average size of the perovskite-type  $A$ -site cation. In  $\text{Bi}_2\text{Sr}_2\text{Nb}_2\text{TiO}_{12}$ , Bi/Sr cation disorder [8] leads to  $\sim 15\%$   $\text{Bi}^{3+}$  ( $IR = 1.17 \text{ \AA}$ ) substitution for  $\text{Sr}^{2+}$  ( $IR = 1.26 \text{ \AA}$ ) on this site, reducing its average size from  $1.26$  to  $1.25 \text{ \AA}$ . In  $\text{Bi}_{1.5}\text{Sr}_{2.5}\text{Nb}_{2.5}\text{Ru}_{0.5}\text{O}_{12}$ , however, all the  $\text{Bi}^{3+}$  cations are located in this  $\text{Bi}_2\text{O}_2$  layer and the  $A$ -site is 100 %  $\text{Sr}^{2+}$ .